Eur J Nucl Med Mol Imaging (2010) 37:1766–1777
DOI 10.1007/s00259-009-1321-8

REVIEW ARTICLE

Small-animal SPECT and SPECT/CT: application in cardiovascular research

Reza Golestani · Chao Wu · René A. Tio · Clark J. Zeebregts · Artiom D. Petrov · Freek J. Beekman · Rudi A. J. O. Dierckx · Hendrikus H. Boersma · Riemer H. J. A. Slart

Received: 18 June 2009 / Accepted: 6 November 2009 / Published online: 13 January 2010
© The Author(s) 2009. This article is published with open access at Springerlink.com

Abstract Preclinical cardiovascular research using noninvasive radionuclide and hybrid imaging systems has been extensively developed in recent years. Single photon emission computed tomography (SPECT) is based on the molecular tracer principle and is an established tool in noninvasive imaging. SPECT uses gamma cameras and collimators to form projection data that are used to estimate (dynamic) 3-D tracer distributions in vivo. Recent developments in multipinhole collimation and advanced image reconstruction have led to sub-millimetre and sub-half-millimetre resolution SPECT in rats and mice, respectively. In this article we review applications of microSPECT in cardiovascular research in which information about the function and pathology of the myocardium, vessels and neurons is obtained. We give examples on how diagnostic tracers, new therapeutic interventions, pre- and postcardiovascular event prognosis, and functional and pathophysiological heart conditions can be explored by microSPECT, using small-animal models of cardiovascular disease.

Keywords microSPECT · microSPECT/CT · Cardiovascular imaging

Introduction

Small-animal models of cardiac disease play an important role in cardiovascular research, and the ability to translate the

Reza Golestani and Chao Wu contributed equally to this work.

R. Golestani · C. Wu · R. A. J. O. Dierckx · H. H. Boersma · R. H. J. A. Slart
Department of Nuclear Medicine and Molecular Imaging, University Medical Center Groningen, Groningen, The Netherlands

R. A. Tio
Thorax Center, Department of Cardiology, University Medical Center Groningen, Groningen, The Netherlands

C. J. Zeebregts
Department of Surgery, Division of Vascular Surgery, University Medical Center Groningen, Groningen, The Netherlands

H. H. Boersma (✉)
Department of Clinical and Hospital Pharmacy, University Medical Center Groningen, Hanzeplein 1, P.O. Box 30001, 9700 RB Groningen, The Netherlands
e-mail: h.h.boersma@apoth.umcg.nl

C. Wu · F. J. Beekman
Image Sciences Institute and Rudolf Magnus Institute of Neurosciences, University Medical Center Utrecht, Utrecht, The Netherlands

A. D. Petrov
Division of Cardiology, School of Medicine, University of California, Irvine, Irvine, California

F. J. Beekman
Faculty of Applied Sciences, Section Radiation Detection and Medical Imaging, Delft University of Technology, Delft, The Netherlands

F. J. Beekman
MILabs, Utrecht, The Netherlands

R. A. Tio · C. J. Zeebregts · H. H. Boersma · R. H. J. A. Slart
Cardiovascular Imaging Group, University Medical Center Groningen, P.O. Box 30001, NL-9700 RB Groningen, The Netherlands

findings to the clinic has been proven in many cases [1–3]. The use of radionuclide imaging in small animals has provided many advantages for researchers to investigate in vivo molecular processes in cardiovascular pathology. Small-animal single photon emission computed tomography (SPECT) systems are now used by many centres for tracer development, therapy evaluation and pathophysiology investigations. Here we discuss the basic principles and preclinical applications of microSPECT and combined microSPECT/CT in cardiovascular research.

Background of microSPECT and microSPECT/CT

SPECT is based on the molecular tracer principle and detection of gamma rays by radiolabelled molecules. The suitable energy range of gamma rays for clinical SPECT is typically around 60–300 keV. Due to the small size of rats and mice, isotopes with much lower energies (e.g. ^{125}I, with 27–35 keV) can be employed in microSPECT, which would not be useful for imaging in patients. For obtaining tomographic images, tens up to hundreds of projection images of the animal are acquired with position-sensitive gamma-detectors. Today almost all small-animal SPECT is performed with pinhole collimators, since these collimators provide a much better noise resolution trade-off in small objects than parallel hole or fan-beam collimators that are commonly used in clinical cardiac SPECT. Most small-animal SPECT systems rotate either the detector and collimator or the object [4–12]. Stationary small-animal pinhole SPECT systems [13–17] do not need to be rotated since they use detector set-ups that cover 360° and many pinholes to provide a large number of projection angles under which the animal is observed. They also have the advantage that dynamic imaging is possible with arbitrarily short frame lengths [15, 18, 19].

The full 360° coverage in combination with many focusing micropinholes and a high magnification factor to maximize the information content per photon provide a very high reconstructed image resolution. Multiple projections from different angles that can be acquired at the same time in such systems facilitate excellent ECG-gated myocardial imaging in rats and mice, which have heart rates of around 300 and 600 beats per minute, respectively. For instance, the U-SPECT-II system (MILabs, The Netherlands) has 75 pinholes on its interchangeable cylindrical collimators (Fig. 1), and is based on three ultralarge NaI scintillation gamma-cameras. Reconstructed images can reach resolutions of ≤0.35 mm and 0.45 mm anywhere in the body using the mouse collimators with 0.35 mm and 0.6 mm gold pinhole apertures, respectively, and ≤0.8 mm with the standard total body rat collimator. It is expected that dedicated high-resolution detectors will contribute to further improvement in multipinhole SPECT resolution, thereby expanding the field of application of microSPECT. In addition, dedicated collimators to image specific organs are under development, and these can dramatically boost performance. Overviews and primers of pinhole SPECT technology have been provided by some investigators [20, 21].

Fig. 1 **a**) Separate U-CT system and U-SPECT-II system. **b**) Integrated U-SPECT-II/CT system

In contrast to PET, dual-tracer or triple-tracer images can be readily obtained with SPECT. Multitracer imaging results in shorter acquisition times and perfect registration of images in space and time, and each tracer represents a different biological process. Another advantage of SPECT is that radiotracers can be produced more easily in the laboratory without the need for a cyclotron, so that the cost-effectiveness of SPECT is higher than that of PET. Clinical PET systems have a much higher resolution than SPECT, but this is reversed for microSPECT since the best resolution of commercial microPET systems is still above 1 mm [22, 23].

Perfusion SPECT provides valuable information for the diagnosis of patients with coronary artery disease (CAD). For example, in triple vessel disease, in which tracer delivery to the whole myocardium is diminished due to

balanced hypoperfusion, SPECT images may be interpreted as normal in qualitative or semiquantitative image analysis because comparison of the defective area with the region of the most intense uptake will not show any difference from normal. Absolute quantification of tracer uptake, which measures megabecquerels of tracer uptake per gram of tissue, can solve this problem [24]. The most prominent obstacles to absolute quantification in clinical SPECT used to be photon absorption and scattering, but today these problems are much smaller: SPECT systems equipped with transmission sources or, more recently, integrated with CT scanners are on the market [25–28]. These allow accurate correction for attenuation, and also use accurate methods to correct for scatter and collimator and detector blurring [29–38]. Cardiac and respiratory movements also degrade quantification, but both could be dealt with through (dual) gating as used in microPET imaging [39]. Although significant technical improvements for absolute quantification of myocardial perfusion using microSPECT have been introduced in recent years, the "roll–off" phenomenon with typical commercial SPECT perfusion agents under hyperaemic conditions, even in humans with less myocardial blood flow than mice, still remains a limitation for accurate measurement in myocardial perfusion imaging.

Quantification errors due to scatter and attenuation do degrade small-animal studies to a much lesser extent than in clinical SPECT because of less photon attenuation in small bodies (about 25% in the centre of a rat body when imaging with ^{99m}Tc [40]). MicroCT imaging is able to provide photon attenuation information which can be used for nonuniform attenuation correction in microSPECT. However, several studies [40, 41] have shown that uniform attenuation correction (which may be based on the animal's body contour) may reduce quantification errors from more than 10% to less than 5%. Therefore, a CT scan that adds dose and needs additional scanning equipment and scan time may be unnecessary. A webcam-based correction has been proposed [41].

Multimodal imaging can rely on separate devices (Fig. 2a) in which images are fused through markers [42, 43], or marker-free methods in which the spatial relationship between beds is known through calibration [42, 44]. The accuracy of registration can be very satisfactory (0.2 mm), and an advantage is that SPECT and CT can be used in parallel, and are individually upgradable. Also registration with other systems such as MRI can be based on the same principles. The advantage and disadvantages of both approaches have been discussed [34, 45].

An attractive aspect of high-resolution integrated micro-SPECT/CT devices [46–49] (e.g. Fig. 2b) is that the bed with the fixed animal does not have to be moved from one scanner to another. Integrated SPECT/CT, in which the bed moves through both the SPECT and the CT scanner is very convenient, although this approach is hard to extend to MRI, and image registration is still needed to obtain accurately matched combined images.

The translatability of the cardiovascular systems of small animals including mice and rats to the human cardiovascular system and the exceptional characteristics of modern microSPECT and multimodality imaging approaches provide promising opportunities in preclinical cardiovascular research. Novel microSPECT systems can provide quantitative images, and can perform longitudinal studies in the same animal, a high pinhole magnification factor resulting in high resolution, possibly dynamic imaging, and multi-tracer imaging. MicroSPECT and microSPECT/CT systems have a wide range of applications in preclinical cardiovascular research, including investigation of myocardial left ventricular (LV) parameters such as ejection fractions and volumes, cardiac innervation parameters, vascular and atherosclerosis parameters, and the timing of administration and dose of novel radiotracers and biomarkers.

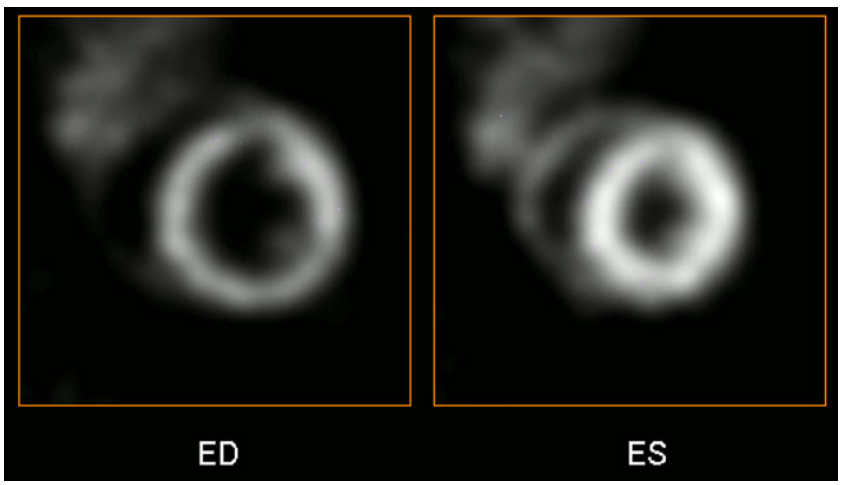

Fig. 2 U-SPECT gated mouse cardiac perfusion images obtained in a normal C57BL/6 mouse (*ED* end diastole, *ES* end systole)

Myocardial applications

Left ventricular function

In order to assess the functional condition of the heart in transgenic mouse models in vivo, small-animal heart imaging can be used for verifying phenotypic differences as well as assessing the benefits of certain therapies. The ability to acquire gated images in small rodents which have high heart rates has eliminated the heart motion effect (Fig. 2). It has been shown that ^{99m}Tc-labelled radiopharmaceuticals, which are routinely used for SPECT imaging in humans, can demonstrate viable tissue and perfusion status in animal models of ischaemia/reperfusion [14]. Further studies have demonstrated that myocardial perfusion defects are correlated with the true size of the defect, and can be analysed quantitatively as well as qualitatively [50, 51]. Liu et al. used animal models of myocardial ischaemia with coronary artery ligation and acquired images after ^{99m}Tc-sestamibi injection. The area where no uptake was seen corresponded with the infarcted tissue which was confirmed by triphenyl tetrazolium chloride (TTC) [14].

Cardiac and respiratory motion can always affect image resolution in SPECT and CT. In order to overcome this problem gating (cardiac and/or respiratory) is performed to synchronize the acquisition of projected data at the same time of the cardiac cycle. Gating also offers the chance to simultaneously map LV perfusion and assess LV function in clinical SPECT applications. ECG-gated microSPECT has been implemented in recent years. It has been shown that preclinical ECG-gated perfusion SPECT (in mice) permits quantification of LV volumes and motion as well. This is also a result of advances in image reconstruction software [52, 53]. The noninvasive nature of the test allows repeated studies in the same animal for follow-up studies [54].

Necrosis visualization

The development of necrotic tissue-avid tracers may help early detection of myocardial infarction (MI) noninvasively. In vivo visualization of necrotic tissue may also provide a quantitative index for evaluating the antinecrotic effect of drugs in development in animal models of ischaemic heart disease.

Glucarate is a small molecular weight compound, a six-carbon dicarboxylic acid sugar, which has affinity for histone proteins. In necrotic cells, due to lesions in the cellular and nuclear membranes, ^{99m}Tc-glucarate can bind to histone proteins and be retained in the tissue [55]. It has been shown that only minimal levels of glucarate bind to normal myocardial cells and viable ischaemic cells. Further studies have illustrated the possibility of immediate postinjection imaging with ^{99m}Tc-glucarate due to its rapid blood clearance [56]. Thus, by using ^{99m}Tc-glucarate as a SPECT tracer, necrotic cells can be depicted to provide data in acute coronary syndrome. Additionally, imaging of infarcts is possible within minutes of occlusion [57–59]. Moreover, it has been shown, by comparative investigations using TTC staining, that SPECT images of ^{99m}Tc-glucarate uptake allow accurate assessment of infarct size. Conversely, it has been shown that there is no glucarate uptake in old necrotic myocardial tissue. Although glucarate uptake in necrotic tissue occurs as early as 3 hours after ischaemia/reperfusion, at 10 days after necrosis there is no obvious tracer uptake in the heart [60].

Some studies have focused on other necrotic tissue-avid tracers than glucarate compounds. Porphyrin derivatives were initially developed as tracers for tumour cell tracking. Reports of the avidity of porphyrin derivatives for necrotic tissue [61–63] and studies on their use in visualization of infarcted tissue by MRI led to efforts to radiolabel hypericin. Hypericin is a natural substance with a biological activity similar to that of porphyrin. Both substances are known to be photosensitizers and have been used in antitumour therapies [64]. Ni et al. synthesized mono-[^{123}I]iodohypericin (MIH) and injected it into rabbit models of MI. SPECT imaging compared to TTC staining and autoradiography confirmed the accumulation of [^{123}I]MIH in the infarcted tissue [65]. In addition, due to the minimal levels of tracer uptake in normal myocardium, the target to nontarget tracer concentration ratio was very high. In another study, Fonge et al. compared the results of [^{123}I]MIH microSPECT with the results of [^{13}N]ammonia microPET in rabbit models of MI. There was a correlation between areas with low blood flow in microPET and [^{123}I]MIH uptake in microSPECT [66].

Apoptosis visualization

Apoptotic cell death has been the subject of many studies investigating opportunities for therapeutic interventions. Apoptosis is an energy-requiring highly regulated form of cell death which is characterized by cell shrinkage, DNA fragmentation, caspase activation, membrane blebbing, and phosphatidyl serine (PS) externalization. It has been demonstrated that reperfusion injury in the heart leads to apoptotic cell death [67–70]. The role of apoptotic cell death in heart failure has also been investigated in many studies [71–73]. The development of radiopharmaceuticals that bind to apoptotic cells has been useful for in vivo evaluation of therapeutic efforts in apoptotic cell death in cardiomyocytes. Annexin A5, a 36-kDa physiological protein, has affinity for binding to the externalized PS. ^{99m}Tc-Annexin A5 has been used as a SPECT tracer in recent years for detecting apoptosis in the preclinical and

clinical settings in vivo. ^{99m}Tc-Annexin A5 uptake has been confirmed by apoptosis-specific immunohistochemistry assays [74–80]. Nevertheless, PS exposure has been shown not to be specific for apoptotic cell death. In necrosis as well, due to leakage in the cell membrane, PS can be exposed and bound to annexin A5. Annexin A5 can visualize apoptotic PS externalization specifically, if used with a second marker showing an intact cell membrane [81].

More recently, a new ^{99m}Tc-bound, PS-avid agent has been developed. The C2A domain of synaptotagmin, which binds to PS in a calcium-dependent manner, has been shown to be sensitive for cell death detection [82]. False-positive uptake, due to some extent to PS exposure in other forms of cell death, led investigations to find more specific tracers for apoptosis visualization. Caspase-3, altered membrane permeability, and several enzymes which are responsible for apoptosis, are appropriate potential targets for apoptosis imaging.

Stem cell therapy evaluation

The recent treatment strategy for cell-death-related heart disease, cellular cardiomyoplasty, needs to be evaluated in preclinical investigations. The most important objectives for the investigations are the optimal cell type, route of delivery, number of cells, suitable timing after infarction, and future monitoring of grafted cells. Imaging modalities may help stem cell therapy in the heart in three ways, including tracking and quantification of transplanted cells, assessment of function and differentiation, and monitoring of underlying tissue status, as well as in assessing the problems involved in the generation of suitable cell materials [83–85]. Zhou et al. used stem cell grafts labelled with ^{111}In-oxyquinoline and performed double tracer ultrahigh resolution SPECT with ^{99m}Tc-sestamibi to evaluate the engraftment of the stem cells in the infarcted area [86]. However, due to the half-life of ^{111}In-oxyquinoline (67.2 h) the imaging could be only done within 96 h of engraftment, and because radioactivity in stem cells remains in the area even after the cells have died, quantification of uptake may overestimate the survival fraction of injected stem cells. Thus, this method may be useful for short-term tracking of the cells and investigating homing strategies for engraftment.

To assess the function of the targeted cells by SPECT, gene imaging can also be used. Gene expression can be assessed by reporter genes. For imaging with a reporter system, a probe is administered to the subject and selectively bound or metabolized with the reported gene product. This interaction results in probe trapping by the transgenic cell and its level is proportional to the gene expression. The result shows the functionality of the cell. One of the reporter genes most used in this regard is herpes simplex virus tyrosine kinase (HSV1-tk), which is absent in mammalian cells and expresses the tyrosine kinase enzyme that converts cytosine to uracil. Hence, only transgenic cells which express this gene can convert 5-fluorocytosine to 5-fluorouracil, and administration of radiolabelled nucleoside to the subject and acquisition with SPECT will show the tracer uptake in the area of cells expressing the reporter gene [87].

A study on tumour cells has shown the sensitivity of the D-isomer of ^{123}I-2′-fluoro-2′-deoxy-1-beta-D-arabinofuranosy-5-iodo-uracil (d-FIAU) in detecting cells positive for HSV1-tk [77]. It has been shown in a study on Wistar rats injected with the adenovirus-expressing hNIS gene that imaging with iodine and technetium tracers can verify the activity of cardiomyocytes [88]. Thus, transferring the gene to the stem cells prior to myocardial cell transplantation can aid the further tracking and monitoring of the graft. Furthermore, for assessment of gene therapy, coexpression of the hNIS gene with the gene of choice has shown promise for future monitoring of cardiac gene therapy. However, one potential obstacle in the use of hNIS for stem cell tracking is gene silencing, which has been reported in neurological studies [85].

Remodelling investigations

LV remodelling after MI leads to LV dysfunction and failure. Matrix metalloproteinase (MMP), a proteolytic enzyme, has been shown to play a causal role in this process [89]. In vivo MMP activation imaging may provide data to quantify and localize MMP activity and its role in further LV remodelling. In addition, MMP imaging provides the opportunity to track therapeutic efforts directed at MMP inhibition to reduce post-MI remodelling. Su et al. investigated the activation of MMP enzymes with microSPECT/CT in mice models of MI. They used a ^{99m}Tc-bound radiotracer (RP805) to visualize MMP in vivo and compared it to in situ zymography, and found a good correlation between the results [90].

The role of blood coagulation factor XIII in post-MI healing has also been studied using ^{111}In-NQEQVSPLTLLK [77]. The noninvasive imaging of factor XIII may help further investigations on the assessment of factor XIII-targeted therapies [91].

Innovative pathophysiology investigations

A better understanding of pathophysiology can shed light on the pathological processes in cardiovascular diseases, and may lead to new therapeutic interventions. Animal models, especially mice and rats, have been used traditionally for the investigation of molecular processes in cardiovascular diseases. Radionuclide imaging has significantly improved our understanding of several aspects of pathophysiology in small

animal models. For instance the role of sigma receptors in cardiomyocytes has been studied in recent years. Their role in blocking the potassium channel and decreasing neuroexcitability in intracardiac neurons has been reported by Zhang and Cuevas [92]. Sigma receptors are a largely unexplored area of cardiology, and should be studied. Recent efforts towards radionuclide imaging of sigma receptors in various organs can be expanded in cardiology to better distinguish sigma receptor function in cardiovascular systems [93].

In another investigation, ^{99m}Tc-losartan was used for noninvasive imaging of angiotensin receptors in mouse heart muscle cells after permanent ligation of the left anterior descending artery [94]. Increased tracer uptake in post-MI hearts and its correlation with remodelling showed the role of the renin-angiotensin axis in progression of heat failure after MI. In addition, this study demonstrated the potential role of noninvasive imaging strategies in identification of patients likely to develop heart failure.

Cardiac innervation imaging

The autonomic nervous system plays an important role in cardiovascular diseases. Disturbances in function and integrity, as well as enhanced sympathetic activity may lead to numerous heart pathologies. Therefore, evaluation of the sympathetic innervation of the heart could provide important data on the aetiology and progress of heart diseases. It might also provide a tool for noninvasive assessment of novel therapeutic approaches targeting sympathetic nervous system activity, and also assessment of the side effects of drugs on cardiac adrenergic function. ^{123}I-labelled metaiodobenzylguanidine (^{123}I-MIBG), an analogue of the false neurotransmitter guanethidine, has been used clinically for sympathetic neuronal activity and integrity since the 1980s. Presynaptic sympathetic nerve terminals can take up and store MIBG in the same way as norepinephrine. Thus, MIBG uptake and washout rate can be influenced by sympathetic tone and the integrity of nerve terminals. Studies using ^{123}I-MIBG in animal models of coronary artery occlusion have revealed more extended nerve damage than myocardial injury in MI [95]. Also, some investigations have focused on the role of denervation in diabetic heart disease and cardiomyopathy [96]. ^{123}I-MIBG uptake defects have also been shown to be related to arrhythmogenesis in the heart after CAD, cardiomyopathy and other cardiac pathologies [97]. Due to more favourable properties of ^{99m}Tc-bound radiopharmaceuticals compared with ^{123}I-based tracers, Samnick et al. labelled 1-(4-fluorobenzyl)-4-(2-mercapto-2-methyl-4-azapentyl)-4-(2-mercapto-2-methylpropylamino)-piperidine (FBPBAT) with ^{99m}Tc and compared its characteristics in the assessment of cardiac adrenergic function in the rat with those of ^{123}I-MIBG [98]. They used rat models pretreated with α1 and β1 inhibitors and acquired SPECT images after radiopharmaceutical incubation. ^{99m}Tc-FBPBAT showed higher uptake than ^{123}I-MIBG. ^{99m}Tc-FBPBAT also had more cardiac adrenergic specificity. Moreover, ^{99m}Tc-FBPBAT targeted postsynaptic adrenoreceptors, whereas ^{123}I-MIBG was absorbed via a presynaptic uptake I route. In another study, the average effective dose of ^{99m}Tc-FBPBAT was shown to be less than half that of ^{123}I-MIBG [99]. These studies encourage further investigations of ^{99m}Tc-based radiopharmaceuticals for SPECT studies of cardiac adrenergic innervation [97].

Vascular applications

Angiogenesis monitoring

Another field of study in ischaemic diseases, including ischaemic heart disease, is the stimulation of angiogenesis in the injured tissue. Angiogenesis is an important process in infarct healing and post-MI LV remodelling. Thus, noninvasive imaging of angiogenesis may improve risk stratification in post-MI patients. Angiogenesis imaging can also provide a tool to evaluate therapeutic interventions aimed at angiogenesis stimulation. Integrins, a family of cell surface receptors, are known to play a role in angiogenesis. αvβ3 integrin-avid agents have been used to visualize angiogenesis in postinfarct animal models. ^{111}In- or ^{123}I-labelled αvβ3 integrin-avid radiotracer has been shown to be focally retained in hypoperfused myocardial regions [58, 100]. Vascular endothelial growth factor (VEGF) also plays a key role in angiogenesis. The radiolabelled antibodies for VEGF have also been used for detecting angiogenesis, especially in tumour cells. Other detectable factors involved in the angiogenesis process, such as activated endothelial cells and MMP, are potential targets for radionuclide imaging of angiogenesis [100].

Plaque imaging

Rupture of atherosclerotic plaque results in severe cardiac events in 70% of acute MIs and sudden cardiac death. Anatomical methods of atherosclerosis imaging visualize coronary artery stenosis, which is responsible for 20% of plaque complications. However, the majority of acute coronary events are a consequence of rupture and further thrombotic occlusion in nonstenotic lesions. Criteria to regard a plaque as rupture-prone and vulnerable have been suggested by Naghavi et al, [101]. The important attributes regarding injury, inflammation, thrombogenicity, proteolysis, stenosis and morphology play a role in the prediction of plaque vulnerability. The major criteria for labelling a

plaque as vulnerable include: active inflammation (monocyte/macrophage and T-cell infiltration), thin cap with large lipid core, superficial platelet aggregation, fissure, and stenosis >90%. Apart from CT-provided data on stenosis, molecular imaging techniques have been widely used in recent years to depict biological processes within plaque regarding other plaque vulnerability criteria as mentioned above [102]. It is particularly noteworthy that the characteristics of the most common type of vulnerable plaque are inflammatory cell infiltration, platelet aggregation, MMP activation, large lipid core content and apoptosis, but not significant stenosis [101]. Thus, addition of molecular imaging techniques to routine plaque assessment procedures can potentially provide better recognition of vulnerable atherosclerotic plaques.

Apoptosis in plaques

Apoptosis is one of the characteristics of a vulnerable atherosclerotic lesion. It has been shown that apoptosis occurs in smooth muscle cells and monocytes in the plaque, and is a good target for visualizing atherosclerotic plaque, in addition to categorizing plaques as vulnerable. In a study on the detection of atheroma in the aorta of balloon-injured rabbits, focal ^{99m}Tc-annexin A5 uptake was shown to be correlated with macrophage apoptosis in the plaque [103].

Isobe et al. demonstrated that SPECT/CT imaging with annexin A5 compounds provides appropriate correlation between tracer uptake and apoptosis in plaques [104]. They showed that in ApoE$^{-/-}$ mice, induced atherosclerotic plaque can be detected by ^{99m}Tc-annexin A5, and the quantitative uptake is related to the macrophage content of the plaque. Reduced ^{99m}Tc-annexin A5 uptake after diet modification and simvastatin therapy has been shown in another study [105].

Thrombogenicity

Thrombosis at the rupture site or the sites of superficial erosions on the plaque is another marker that predicts the vulnerability of plaque. Thrombosis visualization can help predict future events in CAD. Fibrin detection by CT using fibrin-targeted nanoparticles has recently been reported in humans [106]. It can also be used in animal models of cardiovascular diseases to evaluate therapeutic interventions for thrombosis formation and dissolution.

Lipoprotein accumulation

Vulnerable plaques contain more than 40% low-density lipoproteins in their core [101]. ^{99m}Tc-labelled oxidized low-density lipoproteins (oxLDL) allow visualization of lipid accumulation within macrophages and foam cells. Iuliano et al. showed rapid blood clearance and tracer uptake by atherosclerotic plaque in humans [107]. Further studies quantifying tracer uptake and its contribution to the vulnerability of plaques have been performed in small-animal models of CAD [108, 109].

Inflammation

The inflammatory nature of atherosclerosis, due to infiltration of the plaque with macrophages/monocytes and T lymphocytes, provides a target for cell content imaging of atherosclerotic plaques. Interleukin-2 (IL-2), labelled with ^{99m}Tc, was used by Annovazzi et al. to demonstrate T-cell infiltration in human carotid artery atherosclerotic plaques [110]. This study showed the accumulation of tracer in vulnerable plaques and also demonstrated the consequent influence of lipid-lowering on uptake. Circulating monocyte recruitment in the plaque site and lipid phagocytosis by phagocytes have also been studied as approaches to inflammation visualization in atherosclerotic plaques. Although most investigations in this field have been done using microPET, the known advantages of SPECT systems and SPECT specific tracer labelling should stimulate more studies on plaque inflammation by microSPECT.

Proteolysis

Activation of MMP in the atherosclerotic plaque may lead to further instability and rupture. Schafer et al. studied the feasibility of using a ^{123}I-labelled MMP inhibitor in a known model of arterial remodelling and lesion development [111]. They showed that SPECT imaging using [^{123}I] I-HO-CGS 27023A can be an appropriate method for measurement of MMP activity within the plaque. In another study, a ^{99m}Tc-labelled broad MMP inhibitor was used to determine the effects of statin therapy and dietary modification on MMP activation in rabbit models of atherosclerosis [112]. The microSPECT/CT results were compared with histological and immunohistochemical results as well as the results of ex vivo autoradiography, and showed the feasibility of noninvasive MMP activity detection (Fig. 3).

Angiogenesis in plaque

Angiogenesis in atherosclerotic plaque may cause intraplaque haemorrhage and therefore contribute to more risk of plaque rupture. Imaging of angiogenesis with specific tracers which are avid to angiogenic factors, by SPECT or SPECT/CT, can also reveal valuable information on plaque. Imaging of intraplaque haemorrhage, if possible, will also provide valuable information on plaque vulnerability. Davies et al. showed that a proportion of Annexin V uptake in atherosclerotic plaque is due to red blood cell remnants in the plaque after intraplaque haemorrhage [113].

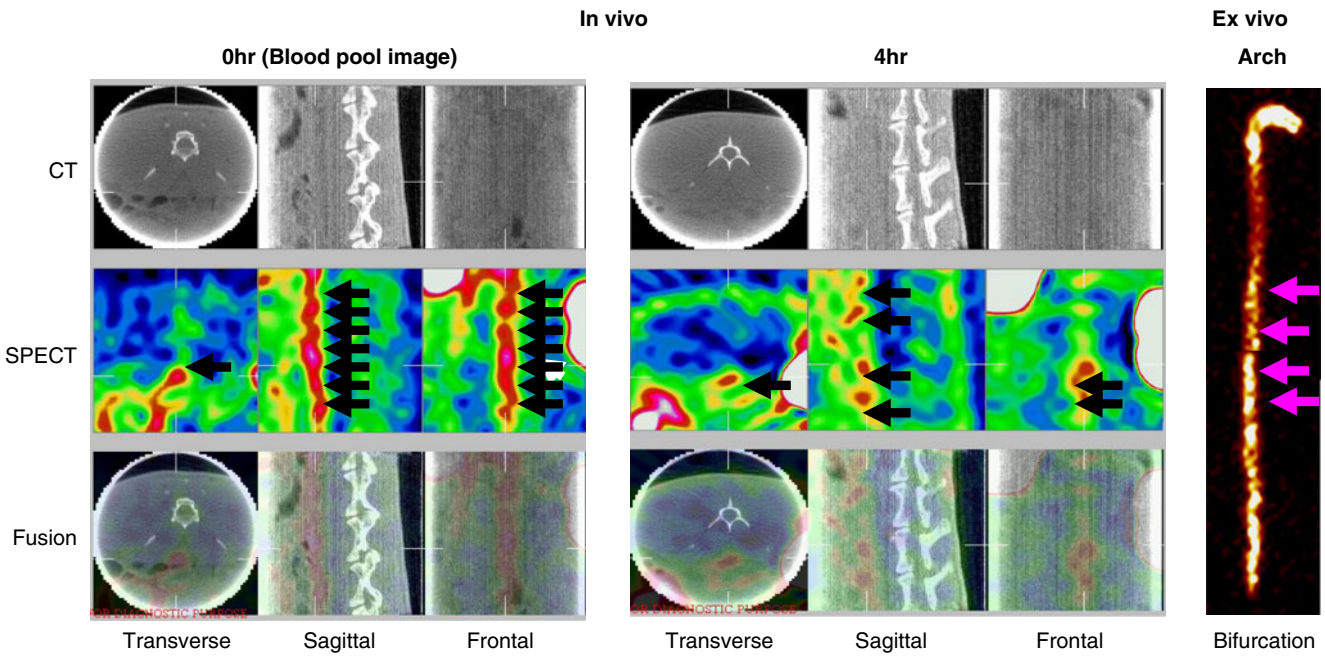

Fig. 3 Uptake of RP805 (a broad-spectrum MMP ligand) demonstrating MMP expression in an atherosclerotic rabbit on an uninterrupted diet. The three columns display transverse, sagittal, and frontal projections, and the three rows display microCT, microSPECT, and fusion images. The left set of three columns displays images immediately (0 h) after radiotracer administration (representing blood pool images), and the right set of three columns displays images obtained at 4 h (representing tracer uptake in target tissue). The images were adapted from reference [74]

However, specific tracers for tracking bleeding within the plaques have not yet been developed.

CT applications

Myocardial application

MicroCT studies of the heart need blood-pool imaging to make the heart contour clear. Iodinated triglyceride is a blood-pool agent that remains in the blood for hours and is cleared slowly through the hepatobiliary systems. This contrast agent, due to its long circulation time, provides the opportunity to select the best postinjection time points for imaging and induces good contrast enhancement between myocardium and blood (500 HU) [114, 115]. Mukundan et al. [116] studied another iodinated agent for microCT which showed more contrast enhancement between myocardium and blood in the LV (650–700 HU). In another study, a novel polymer-coated Bi2S3 nanoparticle (BPNP) was used as contrast agent for CT scanning in mice. This agent showed high stability, high x-ray absorption (fivefold more than that of iodinated agents), and more than 2 hours of circulation time. CT scan of mice using BPNP as contrast agent showed clear delineation of ventricles and vascular structures [117].

In order to evaluate remodelling processes after MI in mouse models, Detombe et al. used retrospective gated microCT [118]. The ability to obtain dynamic images, and short scanning times (<1 min), quantification, and the ability to monitor the same animal during a longitudinal study are promising results of this study. More investigations in the future using hybrid imaging systems (e.g. microSPECT and microCT) will add more dimensions to current preclinical studies.

Vascular dynamics

To investigate the dynamics of myocardial microvessels, $BaSO_4$ contrast microCT has been used for 3-D visualization of the capacitance of intramyocardial vessels during systole and diastole [119]. In this study, the 3-D architecture of microvessels was demonstrated. Images also showed that the vascular volume fraction is decreased from diastole to systole by 48%, but is not collapsed.

Vascular calcification

Atherosclerotic plaque calcification is correlated with total plaque burden and future cardiovascular events [120]. Exploring the underlying pathology of plaque calcification will suggest the direction for future interventions. It has been shown that formation and progression of plaque calcification is correlated with inflammation and apoptosis in atherosclerotic plaques [120, 121]. Interestingly, it has

been shown that microCT can detect plaque calcification in small rodents [104, 122]. Isobe et al. demonstrated the feasibility of microCT images in detecting plaque calcification in the aorta [104]. Although, they used ^{99m}Tc-annexin microSPECT/CT to detect apoptosis in ApoE$^{-/-}$ mice they did not investigate the correlation between calcification and tracer uptake. Further studies using SPECT/CT to correlate different parameters of plaque vulnerability, using SPECT, with calcification, detected by CT, can offer a better understanding on the pathology underlying plaque calcification.

Vascular wall calcification in rodents can also be detected by microCT. In one study on uraemic mice, which have been shown to be a suitable model for vascular calcification, calcification of the aorta was detected and quantified by microCT [123]. The quantification results proved to be reproducible and well-correlated with ex-vivo histological evaluation. This may provide investigators with a promising technique to follow-up and monitor the effects of therapies aiming to reverse vascular calcification in patients with chronic renal failure.

Conclusion

MicroSPECT and microSPECT/CT are powerful tools for elucidating fundamental pathophysiological pathways of heart diseases. They provide information on cardiovascular processes at the molecular and cellular levels. They also offer the opportunity to monitor pharmacological and biological therapeutic interventions in preclinical investigations. Moreover, studies on radiotracer development for detecting new aspects of cardiovascular pathophysiological processes can be investigated in experimental models of cardiovascular pathology. The recent development of hybrid imaging systems, besides providing technical improvements in image quality, adds phenotypic data to functional radionuclide imaging information.

Acknowledgment We thank Ralph Houston for his help during the preparation of the manuscript. The work of R. Golestani was supported by an unrestricted grant from Siemens.

Open Access This article is distributed under the terms of the Creative Commons Attribution Noncommercial License which permits any noncommercial use, distribution, and reproduction in any medium, provided the original author(s) and source are credited.

References

1. Recchia FA, Lionetti V. Animal models of dilated cardiomyopathy for translational research. Vet Res Commun 2007;31(Suppl 1):35–41.
2. Moon A. Mouse models of congenital cardiovascular disease. Curr Top Dev Biol 2008;84:171–248.
3. Franc BL, Acton PD, Mari C, Hasegawa BH. Small-animal SPECT and SPECT/CT: important tools for preclinical investigation. J Nucl Med 2008;49(10):1651–63.
4. Jaszczak RJ, Li JY, Wang HL, Zalutsky MR, Coleman RE. Pinhole collimation for ultra-high-resolution, small-field-of-view SPECT. Phys Med Biol 1994;39:425–37.
5. Ishizu K, Mukai T, Yonekura Y, et al. Ultra-high-resolution SPECT system using four pinhole collimators for small animal studies. J Nucl Med 1995;36:2282–7.
6. Habraken JBA, de Bruin K, Shehata M, Booij J, Bennink R, Smit BLFV, et al. Evaluation of high-resolution pinhole SPECT using a small rotating animal. J Nucl Med 2001;42:1863–9.
7. McElroy DP, MacDonald LR, Beekman FJ, Wang YC, Patt BE, Iwanczyk JS, et al. Performance evaluation of A-SPECT: a high resolution desktop pinhole SPECT system for imaging small animals. IEEE Trans Nucl Sci 2002;49:2139–47.
8. Schramm NU, Ebel G, Engeland U, Schurrat T, Béhé M, Behr TM. High-resolution SPECT using multipinhole collimation. IEEE Trans Nucl Sci 2003;50(3):315–20.
9. Walrand S, Jamar F, de Jong M, Pauwels S. Evaluation of novel whole-body high-resolution rodent SPECT (Linoview) based on direct acquisition of linogram projections. J Nucl Med 2005;46 (11):1872–80.
10. Metzler SD, Jaszczak RJ, Patil NH, Vemulapalli S, Akabani G, Chin BB. Molecular imaging of small animals with a triple-head SPECT system using pinhole collimation. IEEE Trans Med Imaging 2005;24:853–62.
11. Moore SC, Zimmerman RE, Mahmood A, Mellen R, Lim CB. A triple-detector multi-pinhole system for SPECT imaging of rodents. J Nucl Med 2004;45(5):97P.
12. Hesterman JY, Kupinski MA, Furenlid LR, Wilson DW, Barrett HH. The multi-module, multi-resolution system ((MR)-R-3): a novel small-animal SPECT system. Med Phys 2007;34:987–93.
13. Kastis GK, Barber HB, Barrett HH, Gifford HC, Pang IW, Patton DD, et al. High resolution SPECT imager for three-dimensional imaging of small animals (abstract 25). J Nucl Med 1998;39(5 Suppl):9P.
14. Liu Z, Kastis GA, Stevenson GD, Barrett HH, Furenlid LR, Kupinski MA, et al. Quantitative analysis of acute myocardial infarct in rat hearts with ischemia-reperfusion using a high-resolution stationary SPECT system. J Nucl Med 2002;43 (7):933–9.
15. Furenlid LR, Wilson DW, Chen YC, Kim H, Pietraski PJ, Crawford MJ, et al. FastSPECT II: a second-generation high-resolution dynamic SPECT imager. IEEE Trans Med Imaging 2004;51:631–5.
16. Beekman FJ, van der Have F, Vastenhouw B, van der Linden AJA, van Rijk PP, Burbach JPH, et al. U-SPECT-I: a novel system for sub-millimeter resolution tomography of radiolabeled molecules in mice. J Nucl Med 2005;46:1194–200.
17. van der Have F, Vastenhouw B, Ramakers RM, Branderhorst W, Krah JO, Ji C, et al. U-SPECT-II: an ultra-high-resolution device for molecular small-animal imaging. J Nucl Med 2009;50:599–605.
18. Kupinski MA, Barrett HH, editors. Small-animal SPECT imaging. New York: Springer Science+Business Media, 2005.
19. Vastenhouw B, Beekman FJ. Submillimeter total-body murine imaging with U-SPECT-I. J Nucl Med 2007;48:487–93.
20. Beekman FJ, van der Have F. The pinhole: gateway to ultra-high resolution three-dimensional radionuclide imaging. Eur J Nucl Med Mol Imaging 2007;34:151–61.
21. Meikle SR, Kench P, Kassiou M, Banati RB. Small animal SPECT and its place in the matrix of molecular imaging technologies. Phys Med Biol 2005;50(22):R45–61.
22. Visser EP, Disselhorst JA, Brom M, et al. Spatial resolution and sensitivity of the inveon small-animal PET scanner. J Nucl Med 2009;50(1):139–47.

23. Yang Y, Tai YC, Siegel S, et al. Optimization and performance evaluation of the microPET II scanner for in vivo small-animal imaging. Phys Med Biol 2004;49(12):2527–45.
24. Tamaki N, Kuge Y, Tsukamoto E. The road to quantitation of regional myocardial uptake of tracer. J Nucl Med 2001;42:780–1.
25. Even-Sapir E, Keidar Z, Bar-Shalom R. Hybrid Imaging (SPECT/CT and PET/CT) – improving the diagnostic accuracy of functional/metabolic and anatomic imaging. Semin Nucl Med 2009;39:264–75.
26. Seo Y, Mari C, Hasegawa BH. Technological development and advances in single-photon emission computed tomography/computed tomography. Semin Nucl Med 2008;38:177–98.
27. O'Connor MK, Kemp BJ. Single-photon emission computed tomography/computed tomography: basic instrumentation and innovations. Semin Nucl Med 2006;36:258–66.
28. Bockisch A, Freudenberg LS, Schmidt D, Kuwert T. Hybrid imaging by SPECT/CT and PET/CT: proven outcomes in cancer imaging. Semin Nucl Med 2009;39:276–89.
29. Tsui BM, Frey EC, LaCroix KJ, Lalush DS, McCartney WH, King MA, et al. Quantitative myocardial perfusion SPECT. J Nucl Cardiol 1998;5(5):507–22.
30. Beekman FJ, de Jong HW, van Geloven S. Efficient fully 3-D iterative SPECT reconstruction with Monte Carlo-based scatter compensation. IEEE Trans Med Imaging 2002;21 (8):867–77.
31. Zaidi H, Hasegawa B. Determination of the attenuation map in emission tomography. J Nucl Med 2003;44(2):291–315.
32. Bateman TM, Cullom SJ. Attenuation correction single-photon emission computed tomography myocardial perfusion imaging. Semin Nucl Med 2005;35(1):37–51.
33. Hwang AB, Taylor CC, VanBrocklin HF, Dae MW, Hasegawa BH. Attenuation correction of small animal SPECT images acquired with I-125-iodorotenone. IEEE Trans Nucl Sci 2006;53 (3):1213–20.
34. Cherry SR. Multimodality in vivo imaging systems: twice the power or double the trouble? Annu Rev Biomed Eng. 2006;8:35–62.
35. Xiao J, de Wit TC, Staelens SG, Beekman FJ. Evaluation of 3D Monte Carlo-based scatter correction for 99mTc cardiac perfusion SPECT. J Nucl Med 2006;47(10):1662–9.
36. Xiao J, de Wit TC, Zbijewski W, Staelens SG, Beekman FJ. Evaluation of 3D Monte Carlo-based scatter correction for 201Tl cardiac perfusion SPECT. J Nucl Med 2007;48(4):637–44.
37. Hwang AB, Franc BL, Gullberg GT, Hasegawa BH. Assessment of the sources of error affecting the quantitative accuracy of SPECT imaging in small animals. Phys Med Biol 2008;53:2233–52.
38. Hugg J, Uribe J, Jansen F, Manjeshwar R, Laib H, Pang J, et al. A small-animal microSPECT/microCT system with a stationary CZT detector ring and rotating multi-pinhole and multi-slit collimators. J Nucl Med 2006;47(Suppl 1):231P.
39. Yang YF, Rendig S, Siegel S, Newport DF, Cherry SR. Cardiac PET imaging in mice with simultaneous cardiac and respiratory gating. Phys Med Biol 2005;50(13):2979–89.
40. Vanhove C, Defrise M, Bossuyt A, Lahoutte T. Improved quantification in single-pinhole and multiple-pinhole SPECT. Eur J Nucl Med Mol Imaging 2009;36(7):1049–63.
41. Wu C, van der Have F, Vastenhouw B, Dierckx R, Paans A, Beekman F. Absolute quantitative focusing pinhole SPECT. Proceedings of the Tenth International Meeting on Fully Three-Dimensional Image Reconstruction in Radiology and Nuclear Medicine. 5–10 September 2009. Tsinghua University, Beijing, China. p. 291–4. http://www.fully3d2009.org/download/proceedings_2009.pdf. Accessed 20 Nov 2009
42. Chow PL, Stout DB, Komisopoulou E, Chatziioannou AF. A method of image registration for small animal, multi-modality imaging. Phys Med Biol 2006;51(2):379–90.
43. Loening AM, Gambhir SS. AMIDE: a free software tool for multimodality medical image analysis. Mol Imaging 2003;2 (3):131–7.
44. Ji C, Van der Have F, Ramakers R, Beekman FJ. Automatic co-registration of ultra-high-resolution small-animal SPECT with micro-CT images. Submitted.
45. Beekman FJ, Hutton BF. Multi-modality imaging on track. Eur J Nucl Med Mol Imaging 2007;34(9):1410–4.
46. MILabs. U-SPECT/CT. http://www.milabs.com/pages/preclinical-imaging/u-spectct.php. Accessed 20 Nov 2009
47. Bioscan. NanoSPECT/CT in vivo preclinical imager. http://www.bioscan.com/molecular-imaging/nanospect-ct. Accessed 20 Nov 2009
48. Schramm NU, Lackas C, Hoppin JW, Forrer F, de Jong M. The nanoSPECT/CT: a high-sensitivity small-animal SPECT/CT with submillimeter spatial resolution. Eur J Nucl Med Mol Imaging 2006;33:S117.
49. Schramm NU, Lackas C, Gershman B, Norenberg JP, de Jong M. Improving resolution, sensitivity and applications for the NanoSPECT/CT: a high-performance SPECT/CT imager for small-animal research. Eur J Nucl Med Mol Imaging 2007;34: S226–7.
50. Acton PD, Kung HF. Small animal imaging with high resolution single photon emission tomography. Nucl Med Biol 2003;30 (8):889–95.
51. Wu MC, Gao DW, Sievers RE, Lee RJ, Hasegawa BH, Dae MW. Pinhole single-photon emission computed tomography for myocardial perfusion imaging of mice. J Am Col Cardiol 2003;42(3):576–82.
52. Constantinesco A, Choquet P, Monassier L, Israel-Jost V, Mertz L. Assessment of left ventricular perfusion, volumes, and motion in mice using pinhole gated SPECT. J Nucl Med 2005;46:1005–11.
53. Lahoutte T. Monitoring left ventricular function in small animals. J Nucl Cardiol 2007;14(3):371–9.
54. Vanhove C, Lahoutte T, Defrise M, Bossuyt A, Franken PR. Reproducibility of left ventricular volume and ejection fraction measurements in rat using pinhole gated SPECT. Eur J Nucl Med Mol Imaging 2005;32:211–20.
55. Okada DR, Johnson G, Liu Z, Hocherman SD, Khaw BA, Okada RD. Early detection of infarct in reperfused canine myocardium using 99mTc-glucarate. J Nucl Med 2004;45:655–64.
56. Khaw BA, Nakazawa A, O'Donnell SM, Pak KY, Narula J. Avidity of technetium 99 m glucarate for the necrotic myocardium: in vivo and in vitro assessment. J Nucl Cardiol 1997;4:283–90.
57. Khaw BA, Silva JD, Petrov A, Hartner W. Indium 111 antimyosin and Tc-99m glucaric acid for noninvasive identification of oncotic and apoptotic myocardial necrosis. J Nucl Cardiol 2002;9:471–81.
58. Johnson LL, Schofield L, Donahay T, Bouchard M, Poppas A, Haubner R. Radiolabeled arginine-glycine-aspartic acid peptides to image angiogenesis in swine model of hibernating myocardium. JACC Cardiovasc Imaging 2008;1(4):500–10.
59. Narula J, Petrov A, Pak KY, Lister BC, Khaw BA. Very early noninvasive detection of acute experimental nonreperfused myocardial infarction with 99mTc-labeled glucarate. Circulation 1997;95:1577–84.
60. Flotats A, Carrió I. Non-invasive in vivo imaging of myocardial apoptosis and necrosis. Eur J Nucl Med Mol Imaging 2003;30 (4):615–30.
61. Ni Y, Marchal G, Yu J, et al. Localization of metalloporphyrin induced "specific" enhancement in experimental liver tumors: a comparison between MRI, microangiographic and histologic findings. Acad Radiol 1995;2:687–99.
62. Ni Y, Petré C, Miao Y, et al. Magnetic resonance imaging-histomorphologic correlation studies on paramagnetic metalloporphyrins in rat models of necrosis. Invest Radiol 1997;32:770–9.

63. Maurer J, Strauss A, Ebert W, Bauer H, Felix R. Contrast-enhanced high resolution magnetic resonance imaging of pigmented malignant melanoma using Mn-TPPS4 and Gd-DTPA: experimental results. Melanoma Res 2000;10:40–6.
64. Agostinis P, Vantieghem A, Merlevede W, de Witte PA. Hypericin in cancer treatment: more light on the way. Int J Biochem Cell Biol 2002;34:221–41.
65. Ni Y, Huyghe D, Verbeke K, et al. First preclinical evaluation of mono-[123I]iodohypericin as a necrosis-avid tracer agent. Eur J Nucl Med Mol Imaging 2006;33:595–601.
66. Fonge H, Vunckx K, Wang H, et al. Non-invasive detection and quantification of acute myocardial infarction in rabbits using mono-[123I]iodohypericin mSPECT. Eur Heart J 2008;29:260–9.
67. Gottlieb RA, Engler RL. Apoptosis in myocardial ischemia-reperfusion. Ann N Y Acad Sci 1999;874:412–26.
68. Gottlieb RA, Burleson KO, Kloner RA, Babior BM, Engler RL. Reperfusion injury induces apoptosis in rabbit cardiomyocytes. J Clin Invest 1994;94:1621–8.
69. Brady NR, Hamacher-Brady A, Gottlieb RA. Proapoptotic BCL-2 family members and mitochondrial dysfunction during ischemia/reperfusion injury, a study employing cardiac HL-1 cells and GFP biosensors. Biochem Biophys Acta 2006;1757:667–78.
70. Blankenberg FG, Katsikis PD, Tait JF, Davis RE, Naumovski L, Ohtsuki K, et al. In vivo detection and imaging of phosphatidylserine expression during programmed cell death. Proc Natl Acad Sci U S A 1998;95:6349–54.
71. Kang PM, Izumo S. Apoptosis and heart failure: a critical review of the literature. Circ Res 2000;86:1107–13.
72. Blankenberg F, Narula J, Strauss HW. In vivo detection of apoptotic cell death: a necessary measurement for evaluating therapy for myocarditis, ischemia, and heart failure. J Nucl Cardiol 1999;6:531–9.
73. Narula J, Haider N, Virmani R, DiSalvo TG, Kolodgie FD, Hajjar RJ, et al. Apoptosis in myocytes in end-stage heart failure. N Engl J Med 1996;335:1182–9.
74. Hofstra L, Liem IH, Dumont EA, Boersma HH, van Heerde WL, Doevendans PA, et al. Visualisation of cell death in vivo in patients with acute myocardial infarction. Lancet 2000;356:209–12.
75. Narula J, Zaret BL. Noninvasive detection of cell death: from tracking epitaphs to counting coffins. J Nucl Cardiol 2002;9:554–60.
76. Fonge H, de Saint Hubert M, Vunckx K, et al. Preliminary in vivo evaluation of a novel 99mTc-labeled HYNIC-cys-annexin A5 as an apoptosis imaging agent. Bioorg Med Chem Lett 2008;18:3794–8.
77. Shirani J, Dilsizian V. Molecular imaging in heart failure. Curr Opin Biotechnol 2007;18:65–72.
78. Taki J, Higuchi T, Kawashima A, Tait JF, Kinuya S, Muramori A, et al. Detection of cardiomyocyte death in a rat model of ischemia and reperfusion using 99mTc-labeled annexin V. J Nucl Med 2004;45:1536–41.
79. Shan D, Marchase RB, Chatham JC. Overexpression of TRPC3 increases apoptosis but not necrosis in response to ischemia-reperfusion in adult mouse cardiomyocytes. Am J Physiol Cell Physiol 2008;294:C833–41.
80. Boersma HH, Kietselaer BL, Stolk LM, et al. Past, present, and future of annexin A5: from protein discovery to clinical applications. J Nucl Med 2005;46:2035–50.
81. Corsten MF, Reutelingsperger CP, Hofstra L. Imaging apoptosis for detecting plaque instability: rendering death a brighter facade. Curr Opin Biotechnol 2007;18:83–9.
82. Korngold EC, Jaffer FA, Weissleder R, Sosnovik DE. Noninvasive imaging of apoptosis in cardiovascular disease. Heart Fail Rev 2008;13:163–73.
83. Stodilka RZ, Blackwood KJ, Kong H, Prato FS. A method for quantitative cell tracking using SPECT for the evaluation of myocardial stem cell therapy. Nucl Med Commun 2006;27:807–13.
84. Jacob JL, Salis FV, Ruiz MA, Greco OT. Labeled stem cells transplantation to the myocardium of a patient with Chagas' disease. Arq Bras Cardiol 2007;89(2):e10–1.
85. Boersma HH, Tromp SC, Hofstra L, Narula J. Stem cell tracking: reversing the silence of the lambs. J Nucl Med 2005;46:200–3.
86. Zhou R, Thomas DH, Qiao H, et al. In vivo detection of stem cells grafted in infarcted rat myocardium. J Nucl Med 2005;46:816–22.
87. Sharma AK, Dhingra S, Khaper N, Singal PK. Activation of apoptotic processes during transition from hypertrophy to heart failure in guinea pigs. Am J Physiol Heart Circ Physiol 2007;293:H1384–90.
88. Miyagawa M, Beyer M, Wagner B, et al. Cardiac reporter gene imaging using the human sodium/iodide symporter gene. Cardiovasc Res 2005;65:195–202.
89. Creemers E, Cleutjens JP, Smits JF, Daemen MJ. Matrix metalloproteinase inhibition after myocardial infarction: a new approach to prevent heart failure? Circ Res 2001;89:201–10.
90. Su H, Spinale FG, Dobrucki LW, et al. Noninvasive targeted imaging of matrix metalloproteinase activation in a murine model of postinfarction remodeling. Circulation 2005;112:3157–67.
91. Jaffer FA, Sosnovik DE, Nahrendorf M, Weissleder R. Molecular imaging of myocardial infarction. J Mol Cell Cardiol 2006;41:921–33.
92. Zhang H, Cuevas J. sigma Receptor activation blocks potassium channels and depresses neuroexcitability in rat intracardiac neurons. J Pharmacol Exp Ther 2005;313:1387–96.
93. Collier TL, Waterhouse RN, Kassiou M. Imaging sigma receptors: applications in drug development. Curr Pharm Des 2007;13:51–72.
94. Verjans JW, Lovhaug D, Narula N, et al. Noninvasive imaging of angiotensin receptors after myocardial infarction. JACC Cardiovasc Imaging 2008;1(3):354–62.
95. Patel AD, Iskandrian AE. MIBG imaging. J Nucl Cardiol 2002;9:75–95.
96. Langer A, Freeman MR, Josse RG, Armstrong PW. Metaiodobenzylguanidine imaging in diabetes mellitus: assessment of cardiac sympathetic denervation and its relation to autonomic dysfunction and silent myocardial ischemia. J Am Coll Cardiol 1995;25:610–8.
97. Tomoda H, Yoshioka K, Shiina Y, Tagawa R, Ide M, Suzuki Y. Regional sympathetic denervation detected by iodine 123 metaiodobenzylguanidine in non-Q-wave myocardial infarction and unstable angina. Am Heart J 1994;128:452–8.
98. Samnick S, Scheuer C, Münks S, El-Gibaly AM, Menger MD, Kirsch CM. Technetium-99m labeled 1-(4-fluorobenzyl)-4-(2-mercapto-2-methyl-4-azapentyl)-4-(2-mercapto-2-methylpropylamino)-piperidine and iodine-123 metaiodobenzylguanidine for studying cardiac adrenergic function: a comparison of the uptake characteristics in vascular smooth muscle cells and neonatal cardiac myocytes, and an investigation in rats. Nucl Med Biol 2004;31(4):511–22.
99. Richter S, Schaefer A, Menger MD, Kirsch CM, Samnick S. Mapping of the cardiac sympathetic nervous system by single photon emission tomography with technetium-99m-labelled fluorobenzylpiperidine derivative (99mTc-FBPBAT): result of a feasibility study in a porcine model and an initial dosimetric estimation in humans. Nucl Med Commun 2005;26:361–8.
100. Choe YS, Lee K. Targeted in vivo imaging of angiogenesis: present status and perspectives. Curr Pharm Des 2007;13:17–31.
101. Naghavi M, Libby P, Falk E, et al. From vulnerable plaque to vulnerable patient: a call for new definitions and risk assessment strategies: part I. Circulation 2003;108(14):1664–72.

102. Langer HF, Haubner R, Pichler BJ, Gawaz M. Radionuclide imaging a molecular key to the atherosclerotic plaque. J Am Coll Cardiol 2008;52(1):1–12.
103. Kolodgie FD, Petrov A, Virmani R, et al. Targeting of apoptotic macrophages and experimental atheroma with radiolabeled annexin V: a technique with potential for noninvasive imaging of vulnerable plaque. Circulation 2003;108(25):3134–9.
104. Isobe S, Tsimikas S, Zhou J, Fujimoto S, Sarai M, Branks MJ, et al. Noninvasive imaging of atherosclerotic lesions in apolipoprotein E-deficient and low-density-lipoprotein receptor-deficient mice with annexin A5. J Nucl Med 2006;47:1497–505.
105. Hartung D, Sarai M, Petrov A, et al. Resolution of apoptosis in atherosclerotic plaque by dietary modification and statin therapy. J Nucl Med 2005;46(12):2051–6.
106. Winter PM, Shukla HP, Caruthers SD, et al. Molecular imaging of human thrombus with computed tomography. Acad Radiol 2005;12:S9–13.
107. Iuliano L, Signore A, Vallabajosula S, Colavita AR, Camastra C, Ronga G, et al. Preparation and biodistribution of 99m technetium labelled oxidized LDL in man. Atherosclerosis 1996;126(1):131–41.
108. Virgolini I, Rauscha F, Lupattelli G, et al. Autologous low-density lipoprotein labelling allows characterization of human atherosclerotic lesions in vivo as to presence of foam cells and endothelial coverage. Eur J Nucl Med 1991;18:948–51.
109. Iuliano L, Signore A, Violi F. Uptake of oxidized LDL by human atherosclerotic plaque. Circulation 1997;96:2093–4.
110. Annovazzi A, Bonanno E, Arca M, et al. 99mTc-interleukin-2 scintigraphy for the in vivo imaging of vulnerable atherosclerotic plaques. Eur J Nucl Med Mol Imaging 2006;33:117–26.
111. Schafer M, Riemann B, Kopka K, et al. Scintigraphic imaging of matrix metalloproteinase activity in the arterial wall in vivo. Circulation 2004;109:2554–9.
112. Fujimoto S, Hartung D, Ohshima S, et al. Molecular imaging of matrix metalloproteinase in atherosclerotic lesions: resolution with dietary modification and statin therapy. J Am Coll Cardiol 2008;52(23):1847–57.
113. Davies JR, Rudd JH, Weissberg PL, Narula J. Radionuclide imaging for the detection of inflammation in vulnerable plaques. J Am Coll Cardiol 2006;47:C57–68.
114. Badea CT, Drangova M, Holdsworth DW, et al. In vivo small-animal imaging using micro-CT and digital subtraction angiography. Phys Med Biol 2008;53(19):R319–50.
115. Nahrendorf M, Badea C, Hedlund LW, Figueiredo JL, Sosnovik DE, Johnson GA, et al. High-resolution imaging of murine myocardial infarction with delayed-enhancement cine micro-CT. Am J Physiol Heart Circ Physiol 2007;292(6):H3172–8.
116. Mukundan S Jr, Chaghada KB, Badea CT, et al. A liposomal nanoscale contrast agent for preclinical CT in mice. AJR Am J Roentgenol 2006;186(2):300–7.
117. Rabin O, Manuel Perez J, Grimm J, et al. An x-ray computed tomography imaging agent based on long-circulating bismuth sulphide nanoparticles. Nat Mater 2006;5(2):118–22.
118. Detombe SA, Ford NL, Xiang F, Lu X, Feng Q, Drangova M. Longitudinal follow-up of cardiac structure and functional changes in an infarct mouse model using retrospectively gated micro-computed tomography. Invest Radiol 2008;43(7):520–9.
119. Toyota E, Fujimoto K, Ogasawara Y, et al. Dynamic changes in three-dimensional architecture and vascular volume of transmural coronary microvasculature between diastolic- and systolic-arrested rat hearts. Circulation 2002;105(5):621–6.
120. Li JJ, Zhu CG, Yu B, Liu YX, Yu MY. The role of inflammation in coronary artery calcification. Ageing Res Rev 2007;6:263–70.
121. Clarke M, Bennett M. The emerging role of vascular smooth muscle cell apoptosis in atherosclerosis and plaque stability. Am J Nephrol 2006;26:531–5.
122. Ritman EL, Bolander ME, Fitzpatrick LA, Turner RT. Micro-CT imaging of structure-to-function relationship of bone microstructure and associated vascular involvement. Technol Health Care 1998;6:403–12.
123. Persy V, Postnov A, Neven E, Dams G, De Broe M, D'Haese P, et al. High-resolution X-ray microtomography is a sensitive method to detect vascular calcification in living rats with chronic renal failure. Arterioscler Thromb Vasc Biol 2006;26:2110–6.